JAERI-M
6616

SELF-SIMILAR ANALYSIS OF SPHERICAL IMPLOSION PROCESS

July 1976

Y.ISHIGURO and S. KATSURAGI

日本原子力研究所
Japan Atomic Energy Research Institute

JAERI - M 6616

Self-Similar Analysis of the Spherical Implosion Process

Yukio ISHIGURO and Satoru KATSURAGI*

Division of Reactor Engineering, Tokai, JAERI

(Received June 17, 1976)

The implosion processes caused by laser-heating ablation has been studied by self-similarity analysis. Attention is paid to the possibility of existence of the self-similar solution which reproduces the implosion process of high compression.

Details of the self-similar analysis are reproduced and conclusions are drawn quantitatively on the gas compression by a single shock. The compression process by a sequence of shocks is discussed in self-similarity. The gas motion followed by a homogeneous isentropic compression is represented by a self-similar motion.

---

*) Office of Planning, JAERI

JAERI－M 6616

球状爆縮過程の相似解析

日本原子力研究所　東海研究所　原子炉工学部
石黒幸雄・桂木　学*

（1976年6月17日受理）

レーザー加熱による削摩作用で起る爆縮過程を相似解析によって研究した。特に，超高圧縮を伴う爆縮過程を再現する相似解の存在の可能性に注目している。

まず，１つの衝撃波による爆縮過程に対して相似解析の詳細と得られた定量的な結論を示した。相似解析の立場から，多段衝撃波による圧縮についても議論した。さらに，一様な等エントロピー圧縮による気体運動は１つの相似運動であることを示した。

＊　日本原子力研究所　企画室

Contents

I. INTRODUCTION

It is well known that extremely high pressures and temperatures can be achieved by focusing an intense laser pulse on a solid surface. Several plans have been in progress to compress the pellet of thermonuclear fuel to fusioning condition.[1)~5)]

A fraction of the laser light irradiated is absorbed by electrons in the tenuous and hot outer region of the pellet, by the process of inverse bremsstrahrung and various anomalous absorption mechanism. This absorbed energy is then transported inwards to cooler dense region by classical thermal conductivity and is transferred to the pellet ions by classical electron-ion collisions. The high pressure is derived from violent ablation of the strongly-heated surface matter into the vacuum and also from the temperature increments in the thermal front. Being thrusted by the "ablation" piston, shocks are launched toward the pellet center and the unablated portion of the core is compressed to high density.

To achieve extremely high pellet conpression it has been proposed that the laser power should be time-tailored so that the pellet compression takes place nearly isentropically.[1),5)] The high temperature, required to provide an adequate rate of thermonuclear reaction, will be obtained during the compression by a combination of shock heating and compressive work. These phenomena have been inspected by using computer codes based on the detailed hydrodynamic description of plasma fluid.[2),5)]

The behavior of the imploding shock wave was idealized by assuming its dynamics as a self-similar motion[2),6),7)]. In this idealization, use is made of a purely hydrodynamic model without transport processes, that is, with negligible viscosity, thermal conduction, collisional energy exchange and so on. Since monentum, energy and mass flow near the center of the pellet are concentrated in a very small region at the final stage of implosion, the shock intensities should increase greatly. So the shock condition on both the surfaces of a shock may be described approximately by the Rankine-Hugoniot relation for large shock velocities. Extremely rapid changes, caused by the appearance of shock front, in the thermodynamic state of the plasma fluid is approximated in the simple theory by mathematical discontinuities. The total neutron production predicted by the similarity analysis gave an excellent agreement with that obtained from a hydrodynamic computer code[2)].

The physical circumstance predicted by the self-similar motion accompanied by a single shock, however, seems to correspond to a spherical

shock tube problem rather than to an implosion process by strongly accelerating piston. In the former problem, before the spherically contracting shock is reflected at the fluid center, the fluid particle behind the incident shock is moving towards the center. After the reflection, the reflected wave travels in the opposite direction, which is shown to be also a shock. The overall density, pressure, and temperature ratio, produced by the reflection at the center, are considerably increased. This process is known as the so-called "shock and rarefaction wave interactions".[6),7),8)]

On the other hand, for the problem of the strongly accelerating piston, adiabatic compressions will be continuously and unboundedly possible in addition to the shock compression. That is, momentum, energy and mass flow near the fluid center are concentrated in a very small volume at the final stage of implosion, due to the strongly ablating pressure and the spherically focusing effect. Adiabatic compressions lead to much higher densities and much lower temperatures than the corresponding shock compressions. Actually all the computer results show the increasingly growing profiles of density for the shocks which approach the pellet center. However, the compression by a single shock can not lead to higher density than the density at infinity before the shock arrival at the center. Here, it should be noted that the single shock problem can be treated also as a problem of the gas compression by piston moving together with gas. The compression of a pellet may, practically, be accomplished by either of these processes individually, or by some appropriate timed sequence of them[4)].

The primary object of this paper is to discuss the possibility of the existence of the self-similar solution which reproduces the implosion process with laser-heated ablation. The impoding shocks were analysed by Guderly[9)] but the literature is not available in this country yet. Hence, the actual details of the self-similar analysis will at first be reproduced in the next section by following Sedov[5)]. Next, discussions will be made on the correspondency to the practical implosion processes and also on the possibility of the existence of the self-similar solution. Additionally the problems related to the way to produce extremely high compression will be touched on from the standpoint of the self-similar motion.

II. SELF-SIMILAR MOTION

We assume that the the target plasma is fully ionized and the relaxation time between the electron and ion collision is so short that the plasma can be treated with one-component neutral perfect gas. Moreover, the disturbance in fluid induced by the fusion reaction is assumed to be negligible. Then, the equations of motion, continuity and energy take the form:

$$\left.\begin{aligned} &\frac{\partial v}{\partial t} + v\frac{\partial v}{\partial r} + \frac{1}{\rho}\frac{\partial p}{\partial r} = 0, \\ &\frac{\partial \rho}{\partial t} + \frac{\partial \rho v}{\partial r} + (\nu - 1)\frac{\rho v}{r} = 0, \\ &\frac{\partial}{\partial t}\left(\frac{p}{\rho^{\gamma}}\right) + v\frac{\partial}{\partial r}\left(\frac{p}{\rho^{\gamma}}\right) = 0, \end{aligned}\right\} \tag{1}$$

where γ is the adiabatic index; $\nu = 1$ for plane flow, $\nu = 2$ for flow with cylindrical symmetry, and $\nu = 3$ for flow with spherical symmetry.

From dimensional analysis for the velocity v, density ρ and pressure p, we can write[6)]

$$v = \frac{r}{|t|}V(\lambda), \quad \rho = \frac{a}{r^{k+3}|t|^{s}}R(\lambda), \quad p = \frac{a}{r^{k+1}|t|^{s+2}}P(\lambda) \tag{2}$$

where V, R and P are arbitrary quantities depending only on the non-dimensional combination of r and t, and

$$\lambda \equiv \frac{r}{b|t|^{\delta}} \quad . \tag{3}$$

Here, the constants, a and b have the following dimensions, respectively:

$$[a] = ML^{k}T^{s} \qquad \text{and} \qquad [b] = LT^{-\delta}. \tag{4}$$

Substituting Eq. (2) into Eq. (1) and introducing the new variable

$$Z = \gamma P/R, \tag{5}$$

we obtain[6)]

$$\frac{dZ}{dV} = \frac{Z\{[2(V\mp1)+\nu(\gamma-1)V](V\mp\delta)^2 - (\gamma-1)V(V\mp1)(V\mp\delta) - [2(V\mp1)\mp\kappa(\gamma-1)]Z\}}{(V\mp\delta)[V(V\mp1)(V\mp\delta)-(\nu V\mp\kappa)Z]} , \quad (6)$$

$$\frac{d\ell n\lambda}{dV} = \frac{Z-(V\mp\delta)^2}{V(V\mp1)(V\mp\delta)-(\nu V\mp\kappa)Z} . \quad (7)$$

$$(V\mp\delta)\frac{d\ell nR}{d\ell n\lambda} = \pm S + (k-\nu+3)V - \frac{V(V\mp1)(V\mp\delta)-(\nu V\mp\kappa)Z}{Z-(V\mp\delta)^2} , \quad (8)$$

with $$\kappa \equiv \frac{S + 2 + \delta(k+1)}{\gamma} , \quad (9)$$

where the upper and lower signs correspond, respectively, to the implosion ($t<0$) and explosion ($t>0$) processes.

The two parameters, a and b, and the nondimensional constants, k, s and δ are determined depending on the physical problem under consideration. For the example of the implosion process (spherical shock tube problem), an infinitely strong shock wave is contracting in an undisturbed uniform medium of density ρ_0 and zero pressure. The medium within $r < r_0$ is assumed to be at rest before the instant $t = -t_0$ ($t_0 > 0$) the shock arrives at $r = r_0$. By letting $k = -3$ and $s = 0$, we have $a = \rho_0$ and δ remains to be determined later, but the choice of b is not essential in this problem.

Now, the fundamental problem reduces to the integration of Eq. (6). If Eq. (6) is integrated, then the relations of V and R to λ are determined from Eqs. (7) and (8) by using a numerical integration. A certain curve obtained in the (Z,V) plane gives the field of one-dimensional unsteady motion at each instant. Points of discontinuity on this curve will represent the shocks in the presence of strong explosions or implosions. From Eq. (7), a certain λ-value will correspond to each point of the discontinuities. Hence, the surface of discontinuity in physical space is given by

$$\lambda = \lambda_0 = \text{const}, \qquad r = \lambda_0 b|t|^{\delta} . \quad (10)$$

That is, fixed values of the variables λ, V, Z, R and P correspond to a shock in self-similar motions.

The magnitude of the shock velocity c is given by

$$c = \frac{dr}{dt} = \delta \frac{r}{t} \quad . \tag{11}$$

For the present problem, the shock coordinate can be written as follows:

$$\frac{r}{r_0} = \left(\frac{|t|}{t_0}\right)^{\delta} \frac{\lambda^*}{\lambda_0} \quad \text{or} \quad \frac{r}{c_0 t_0} = \frac{1}{\delta} \left(\frac{|t|}{t_0}\right) \frac{\lambda^*}{\lambda_0} \tag{12}$$

with $\lambda_0 \equiv \frac{r_0}{b t_0^{\delta}}$,

where λ^* is λ_0 for $t < 0$ and a constant determined by shock conditions for $t \geq 0$.

Thus, for the self-similar motion, we can obtain particular solutions by the integration of a single ordinary differential equation (6). It may turn out that by varying the arbitrary constants of the fundamental equations, (6), (7) and (8), it is possible to construct a variety of solutions describing all possible motions of the gas. It should be noted that self-similar solutions provide a physical rather than a mathematical picture.

II.-1 SHOCK CONDITIONS

In the problem under study, discontinuities or shocks occur in the flow; consequently, we must know the general relations between V, Z and R on both sides of a surface of strong discontinuity. On doing so, we simplify the structure of shock front by a mathetical discontinuity neglecting its thickness.

The conditions for conservation of mass, momentum and energy must be satisfied when the fluid crosses a surface of discontinuity. Let the subscripts 1 and 2 denote the states on one side and the other side of the discontinuity, respectively. Then, we can write:

$$\left.\begin{aligned} &\rho_1(v_1 - c) = \rho_2(v_2 - c) \\ &\rho_1(v_1 - c)^2 + p_1 = \rho_2(v_2 - c)^2 + p_2 \\ &\frac{1}{2}(v_1 - c)^2 + \frac{\gamma}{\gamma-1}\frac{p_1}{\rho_1} = \frac{1}{2}(v_2 - c)^2 + \frac{\gamma}{\gamma-1}\frac{p_2}{\rho_2} \end{aligned}\right\} \tag{13}$$

Especially for the case where the state 1 is an undisturbed gas ($v_1 = 0$, $t < 0$), we have

$$\left.\begin{aligned} \frac{v_2}{c} &= \frac{2}{\gamma+1}(1 - M_1^{-2}) \ , \quad \frac{\rho_2}{\rho_1} = \frac{\gamma+1}{\gamma-1}(1 + \frac{2}{\gamma-1} M_1^{-2})^{-1} \\ \frac{p_2}{\rho_1 c^2} &= \frac{2}{\gamma+1}(1 - \frac{\gamma-1}{2\gamma} M_1^{-2}) \end{aligned}\right\} \tag{14}$$

where M is the Mach number defined by

$$M_1 = \frac{c}{c_s} \qquad \text{with} \qquad c_s^2 = \frac{\gamma p_1}{\rho_1} \ . \tag{15}$$

By replacing the quantities v, ρ and p in Eqs. (13) and (14) by means of Eqs. (2), (5) and (11), the relations of Eqs. (13) and (14) at a shock front become, respectively,[6] as

$$\begin{aligned} & R_1(V_1 \mp \delta) = R_2(V_2 \mp \delta) \ , \\ & V_2 \mp \delta = (V_1 \mp \delta)[1 + \frac{2}{\gamma+1} \frac{Z_1 - (V_1 \mp \delta)^2}{(V_1 \mp \delta)^2}] \ , \\ & Z_2 = (\frac{\gamma-1}{\gamma+1})^2 \frac{1}{(V_1 \mp \delta)^2} [(V_1 \mp \delta)^2 + \frac{2Z_1}{\gamma-1}][\frac{2\gamma}{\gamma-1}(V_1 \mp \delta)^2 - Z_1] \end{aligned} \tag{16}$$

and

$$\left.\begin{aligned} V_2 &\cong -\frac{2\delta}{\gamma+1} \ , \qquad R_2 \cong \frac{\gamma+1}{\gamma-1} \\ Z_2 &\cong \frac{2\gamma(\gamma-1)\delta^2}{(\gamma+1)^2} \end{aligned}\right\} \tag{17}$$

where the terms of the order of M_1^{-2} are neglected in deriving Eq. (17) under the assumption of extremely strong shock.

Knowing the state 1 on one side of a surface of discontinuity, we can find from Eq. (16) the state 2 on the another side. In other words, the integral curves in the (V, Z) plane are discontinuously connected, corresponding to the states of both the sides of shock, by the relations of Eq. (16). It should be noted that the subscripts 1 and 2 in Eq. (16) can be interchanged from the symmetry of Eq. (13).

From Eq. (16), the following useful transformations exist between the states 1 and 2 in the (V, Z) plane[6]"

(i) The points on

$$Z = (V \mp \delta)^2 \tag{18}$$

transform into themselves.

(ii) The points on $Z = 0 \Rightarrow Z = \frac{2\gamma}{\gamma-1}(V \mp \delta)^2$. (19)

(iii) The points on $V = 0 \Rightarrow Z = \mp\delta(V \mp \delta)(1 \mp \frac{\gamma-1}{2\gamma} V)$. (20)

(iv) $\frac{\rho_2}{\rho_1} = \frac{R_2}{R_1}$ or $(V_1 \mp \delta)(V_2 \mp \delta) > 0$. (21)

The figure 1 shows the possible transformations, for $t > 0$, given by Eq. (16). The transformation of Eq. (17) is a special case of Eq. (16). That is, Eq. (17) corresponds to the jump from the origin ($V = 0$, $Z = 0$) to the (V_2, Z_2) that is the intersection of two parabolas of Eqs. (18) and (19) with positive sign.

III. INTEGRAL CURVES IN (V, Z)-PLANE FOR SPHERICAL SHOCK-TUBE PROBLEM

For all the problems concerning the implosion process followed by an explosion process, we must look for the unique solutions of V, Z and R that are in one-by-one correspondence with the λ-values in the ranges from the initial value λ_0 to ∞ for $t < 0$ and from ∞ to 0 for $t > 0$. Under the assumption of the strong shock of Eq. (14) or (17), the state of pellet core in the (V, Z) plane corresponds to the origin (V = 0, Z = 0) before the instant when the shock arrives at the space point of observation. Immediately after the arrival of the shock, the fluid state jumps to a point given by Eq. (17), which is the initial condition of the ordinary differential equation (6).

In this section discussion is made on various singular points, that is, discontinuities of the integral curves of Eq. (6) and on the correspondency with the physical state of the imploding or exploding fluid. A set of the unique solutions are obtained for the quantities V, Z and R, which satisfy the physical condition of the spherical shock tube problem. Some of the conclusions drawn are applicable also to other types of implosion process.

III.-1 CONTINUITY OF PHYSICAL STATE AT $t = \pm 0$

From the definition of the parameter λ by Eq. (3), the quantities V, Z and R at $\lambda = \infty$ represent the state at infinity ($r = \infty$) or $t \to \pm 0$. For $t \to \pm 0$, i.e., $\lambda \to \infty$, all the physical quantities must be bounded, possibly except for the center of symmetry ($r = 0$). For an example, from Eq. (2) the integral curve of $V(\lambda)$ must satisfy the following condition:

$$V(\lambda) \to C_V^0 \lambda^{-\frac{1}{\delta}} \quad \text{for} \quad \lambda \to \infty (t \to \pm 0), \tag{22}$$

where C_V^0 is an arbitrary constant. The above equation shows that the physical state at $t \to \pm 0$ corresponds to a point on the Z-axis (V = 0).

The point O (V = 0, Z = 0) is a singular point of Eq. (6)[2),10)]. That is to say, for $V \to 0$ and $Z \to 0$ simultaneously, we have

$$\frac{dZ}{dV} \cong \frac{2Z}{V \pm \frac{\kappa}{\delta} Z} \quad . \tag{23}$$

The general solution of the above equation can be written as

$$V \mp \frac{\kappa}{\delta} Z = CZ^{1/2} \tag{24}$$

the shock point and arrives at the point O passing through the saddle point exists only for one special value of δ. We obtained the special value of δ by an iteration method based on try-and-error procedure. On this method, starting from an assumed value of δ, the slope at the saddle point is determined and a numerical integration starts along the slope towards the shock point. The δ-value sought is that for which the integral curve passes just through the shock point.

Generally, an integral curve which starts from a certain point near any singular point cannot be calculated by a usual numerical procedure such as the Runge-Kutta method, because the function $Z(V)$ is not always a single-valued function of V. We adopted a numerical method to find the next mesh-point on the integral curve by the use of the tangential line and the curvature, as shown in Fig. 3.

As the special value of δ, we obtained $\delta = 0.68829$ for $\gamma = 5/3$. A typical example of the family of integral curves near the saddle point is shown in Figs. 4 and 5. At this step, the constant C_o in Eqs. (26) and (29) is already fixed.

III.-3 INTEGRAL CURVE FOR EXPLOSION PROCESS ($t > 0$).

According to the continuity condition at $t \to 0$, the integral curve for $t > 0$ starts, in the negative half plane of V, from the point O along the parabola of Eq. (29). Before intersecting the parabola of Eq. (20) with minus sign, the curve encounters a discontinuity corresponding to the reflected shock. The image point of the discontinuity transforms into a certain point in the region where $V > 0$ by a jump given by Eq. (16). This point can be determined by considering the final state of the explosion process, and the procedure of the determination will be shown below.

The final state where $t \to +\infty$ or $r \to 0$ is expressed by one certain point in the (V, Z) plane which corresponds to $\lambda = 0$. The point

$$D\left(V = \frac{\kappa}{\nu},\ Z = \frac{C_B}{V - \frac{\kappa}{\nu}} \to \infty\right) \tag{36}$$

is a saddle point, where C_B is a constant defined by

$$C_B = \frac{\kappa(\kappa-\nu)(\kappa-\nu\delta)^2}{\nu^3[\kappa(2+\nu\gamma) - \nu(2+\nu\delta)]} \tag{37}$$

which is obtained by substituting Eq. (36) into Eq. (6). The following asymptotic formulas are valid near the point D:

$$V = \frac{\kappa}{\nu} + C_V \lambda^{C^*} \quad , \qquad Z = C_z \lambda^{-C^*} \quad , \tag{38}$$

with
$$C^* = \frac{\kappa(\kappa-\nu)(\kappa-\nu\delta) - \nu^4 C_B}{\nu^3 C_B} = \frac{\kappa[2+\nu(\gamma-1)] - 2\nu}{\kappa - \nu\delta} \quad , \tag{39}$$

$$R = C_r \lambda^{C^{**}} \quad , \quad \text{where} \quad C^{**} = \frac{\kappa}{\nu\delta-\kappa} \tag{40}$$

$$P = C_p \lambda^{-2} \quad . \tag{41}$$

Here, the constants C_V, C_z, C_r and C_p can be determined later by the numerical integration of Eqs. (7) and (8).

Consequently, the differential equation (6) is integrated starting from the point D of Eq. (36). After intersecting the parabola of Eq. (20) with negative sign, we can construct a curve in the region of $V < 0$ which is the locus of the image points made by the transformation of Eq. (16) for the points on the integral curve. This locus will intersect the integral curve starting from the point O at a certain point in the region of $V < 0$. It is the intersection that we seek as the jump point corresponding to the reflected shock. The integral curve thus obtained is shown in Fig. 6.

III.-4 NUMERICAL RESULTS AND DISCUSSIONS

We can obtain the λ-dependence of the quantities, V, R, Z and P by integrating Eqs. (7) and (8) along the integral curves obtained in the previous subsections. The Runge-Kutta method was used for the purpose of the numerical integrations.

Now, let us consider a shock wave that passed the point $r = r_0$ at $t = -t_0 < 0$ and assume $\lambda = 1$ at this shock point (V_2, Z_2). Then, starting from the this point with $\lambda = 1$, Eqs. (7) and (8) are integrated up to the point near O, along the integral curve of Fig. 5. It is useful to use the asymptotic formulas of Eqs. (22), (29), and (30) in the vicinity of the point O.

For the explosion process ($t > 0$), the integration starts from the point O along the curve given by the analytic expressions of Eqs. (22) and (30) and is accomplished, along the curve of Fig. 6 ($V < 0$), up to the shock point of the reflected wave. The value of λ corresponding to the reflected shock point determines the magnitude of the reflected shock velocity (see Eqs. (11) and (12)). For the jump to the region of $V > 0$,

the shock condition of Eq. (16) for R is used. Here, the value of λ must naturally be treated as a smoothly increasing variable.

The integrated results are shown in Figs. 7-10. From these results, the dimensional quantities v, ρ, and p can be calculated by using Eq. (2). In this case, the following non-dimensional representation of these quantities is much convenient for the general discussions made later:

$$\frac{v}{c_0} = \frac{1}{\delta} \frac{r'}{t'} V(\lambda), \tag{42}$$

$$\frac{\rho}{\rho_0} = R(\lambda) , \tag{43}$$

$$\frac{p}{\rho_0 c_0^2} = \frac{1}{\delta^2} \left(\frac{r'}{t'}\right)^2 P(\lambda), \tag{44}$$

with $$c_0 \equiv \delta \left(\frac{r_0}{t_0}\right) , \tag{45}$$

where r' and t' are the reduced distance and time, respectively, defined by

$$r' \equiv r/r_0 \qquad \text{and} \qquad t' = t/t_0 . \tag{46}$$

Figures 11 $\sim$ 15 show the various profiles of the reflection of a shock at r = 0, as function of time: The reflected shock needs about 1.5 times as much time for the distance 0 and r_0 compared with the incident shock. The fluid follows slowly after the reflected shock. The passage of the incident shock gives a density increase of a factor of four by the shock compression, followed by adiabatic compression of the inwardly moving gas to a density ratio of about 15. The density ratio produced on the reflection is increased by as much as a factor of 33. This is the maximum compression that can be achieved in spherical geometry by passage of one single shock.

The spatial distributions of the various quantities for t > 0 are shown in Figs. 16 $\sim$ 18. The distribution for t < 0 may be inferred from Figs. 7 $\sim$ 9. For example, the density distribution is an properly shrunk profile of the curve for t < 0 in Fig. 9.

It should be noted that for t < 0 the density ratio of the contracting gas to the startionary one is always lower than that of the gas at infinity. Hence, this gas motion corresponds just to that after the passage of the shock in the shock tube. Figure 19 shows the radius of the gas particles versus time until the reflection. The gas moves towards the center of

pellet along the comparatively straight particle-lines. This gas motion can be represented by a gas motion derived by a piston which moves along one of the particle lines. Other motions of piston may derive non-self-similar motions.

Figure 9 shows that a gas compression beyond the compression ratio of about 10 is impossible for $t < 0$ by a single shock. Numerical results obtained from a compter simulation show that the gas density grows increasingly with the approach to the gas center. In the next section, discussions are made on the possibility that such a gas motion can be expressed by a self-similar motion.

IV. SELF-SIMILAR MOTION IN IMPLOSION PROCESS WITH HIGH COMPRESSION

There are two basic ways in which laser-induced ablation pressure can be employed to produce extremely high compression, which represent opposite limits. The first way is to use the strong spherically convergent shock (S), which was discussed by making use of the self-similar analysis in the previous section. The second is based on the shockless or isentropic compression (I). Kidder presented the analytic theory of homogeneous isentropic compression in which every volume element is compressed to the same degree.[4] The compression of a pellet may, in general, be accomplished by either of these processes individually, or by some appropriately timed sequence of them such as[4]:

(S,S), (S,I), (S,S,S), (S,I,S) ·····

In this section we shall examine the possibility that the kinematics of the implosion is reproducible by the self-similar motion. In this case, we shall confine our attention to the following two sinple cases: They are the compression accomplished by a sequence of shocks (S,S,S,·····), and the homogeneous isentropic compression which was discussed by Kidder in the Lagrangian description[4].

IV.-1 IMPLOSION BY A SEQUENCE OF SHOCKS

At first, we assume that the shocks are timed to arrive together at the center of pellet. This compression model is similar to the Beker's model for the formation of shock wave by coalescence of pressure pulses.[8] For a sequence of spherically contracting shocks, it is possible for them to be united at the center by optimizing the strength on a fixed space point of pellet. For this implosion process to be discribed by a self-similar motion, the motion after each shock must be also the self-similar motion.

Let us assume that the first contracting-shock proceeds in unperturbed gas and its strength is so strong that the process can be described by a self-similar motion discussed in the previous section. Moreover we assume that the second shock is launched toward the center in the gas flow after the first shock. The motion of the second shock corresponds to a certain point on the locus of the image points which are given by the transformation of Eq. (6) from the points on the integral curve (see Fig. 20). The integral curve representing the gas motion after the second shock is to be given by a smooth curve that starts from the shock point and arrives at the point O (V = 0, Z = 0). In order that both the motions are self-similar,

both the shock parameters, δ's, must be the same. In the previous section, it was shown that only one integral curve can traverse the parabola of Eq. (18) with a certain slope when the δ-value is fixed. It will be seen from Fig. 20 that two successive shock-motions with the same δ-value can be self-similar only for two trivial cases; the first case corresponds to the identical transformation on the saddle point given by Eq. (34) and the second to the transformation from the point 0 on which the first shock is about to arrive at the center. Consequently, the implosion process accompanied by a sequence of shocks is impossible to be a self-similar motion, at least under the assumption that the gas state is uniform before the shock arrival and the contracting shock is extremely strong.

IV.-2 BREAKDOWN OF SELF-SIMILARITY

It is meaningful to discuss the initial gas state from the standpoint of the self-similarity analysis. Here, it is again assumed that the gas is initially at rest. Substituting the general equation (2) into Eq. (1) and letting $V = 0$ in the resultant equations, we have for $t < 0$

$$-\delta\lambda\left(\frac{P'}{P} - \gamma\frac{R'}{R}\right) = (1-\gamma)S + 2 \quad , \tag{47}$$

$$\lambda P' = (k+1)P \quad , \tag{48}$$

$$\lambda\delta\frac{R'}{R} = -S \quad . \tag{49}$$

The above equations have, respectively, the following solutions:

$$\frac{P}{R^{\gamma}} = C_1\lambda^{-\frac{(1-\gamma)s+2}{\delta}} \quad , \tag{47'}$$

$$P = C_2\lambda^{(k+1)} \tag{48'}$$

$$R = C_3\lambda^{-\frac{s}{\delta}} \quad , \tag{49'}$$

which give a relation among the shock parameters:

$$k+1 + \frac{s+2}{\delta} = 0 \quad \text{or} \quad \kappa \equiv 0 \quad . \tag{50}$$

Making use of Eqs. (2), (48'), (49') and (50), the density and pressure is given by

$$\rho = a r^{\frac{2}{\delta} - 2} \quad ; \quad p = p_1 \quad \text{const.} \tag{51}$$

Hence, the initial gas state with uniform entropy and null velocity may generally have a spatial dependence of the density. That is, the self-similarity requires that the collapsing pellet somewhat resembles a hollow shell. A constant density is attainable only for the case of $\delta = 1$, under the treatment of the self-similarity analysis. Therefore the self-similarity is considered to be violated on the boundary between shock and unperturbed gas in the treatment of the previous sections.

On the other hand, immediately before the instant of the shock arrival, the gas state is represented by a certain point on the V-axis, i.e.,

$$Z_1 \equiv \frac{\gamma P_1}{R_1} = \frac{\gamma p_1}{\rho_1} \frac{t^2}{r^2} \quad . \tag{52}$$

Here, since the shock position and the initial density are given respectively by Eqs. (12) and (51), the Z_1 takes a constant value.

Therefore, the self-similarity holds for all the values of t and r only when the δ-value of the unperturbed gas is the same as that of the gas in motion. It will be seen from the above equation that a constant Z_1-value means that the Mach number of the flow is independent of time.

The theory discussed here strictly applies only to the somewhat artificial situation in which the density increases with radius according to Eq. (51). Such a situation was already studied by Kidder, in connection with homogeneous isentropic compression[4]. This problem has not been treated from the standpoint of the self-similarity analysis and will be discussed in a separate paper in near future.

IV.-3 "HOMOGENEOUS" ISENTROPIC COMPRESSION

Kidder studied homogeneous isentropic compression, i.e., an isentropic compression in which every volume element is compressed to the same degree[4]. It was shown that a close approximation to compression of this type may be accomplished by light-induced pellet ablation if the light absorbed by the pellet is properly programmed with time.

Thus, in a homogeneous compression, the volume element d^3x in the Lagrangian description is assumed to decrease everywhere at the same rate, i.e.,

$$r^2 dr = h^3(t) r_0^2 dr_0$$

or

$$r(r_0, t) = r_0 h(t) , \tag{52}$$

where h(t) is a dimensionless scale factor.

From the law of mass convervation we may write

$$dm = \rho r^2 dr = dm_0 = \rho_0 r_0^2 dr_0 , \tag{53}$$

which, together with Eq. (52), implies that

$$\rho(r_0, t) = \rho_0(r_0)/h^3(t) . \tag{54}$$

Moreover assuming the relation between pressure and density of an ideal gas, we can write

$$\begin{aligned} p(r_0, t) &= a(r_0)\rho^\gamma(r_0, t) \\ &= p_0(r_0)/h^{3\gamma}(t) . \end{aligned} \tag{55}$$

The time-dependent shrinking factor h(t) can be obtained by making use of Eqs. (52), (54) and (55), and separating variables in the equation of motion. The resultant expression can be written as follows[4]:

$$h(t) = [1 - (1 - \frac{|t|}{t_0})^2]^{1/2} \qquad (t < 0) , \tag{56}$$

where the fluid is assumed to be initially at rest and in motion at the time $t = -t_0 < 0$.

The radial dependence of the initial density $\rho_0(r_0)$ and pressure $p_0(r_0)$ can be obtained solving the spatial part of the equation of motion written in the form of the separation of variables[4]:

$$\rho_0(r_0) = \rho_0(0)(1 + \beta x_0^2)^{3/2} , \tag{57}$$

$$p_0(r_0) = p_0(0)(1 + \beta x_0^2)^{5/2} , \tag{58}$$

$$\beta = (R_0/c_s t_0)^2/3 , \quad x_0 = r_0/R_0 < 1 , \tag{59}$$

$$c_s^2 = \gamma p_0(0)/\rho_0(0) . \tag{60}$$

If the compression takes palce slowly ($\beta \ll 1$), we see that the compressed pellet is spatially uniform, i.e.,

$$\rho_0(r_0) \cong \rho_0(0), \qquad p_0(r_0) \cong p_0(0) \quad . \tag{61}$$

On the other hand, rapid homogeneous compression ($\beta \gg 1$), however, requires that the density and pressure increase strongly with radius, according to

$$\rho_0(r_0) \cong \rho_0(0)\beta^{3/2}x_0^3 \ , \quad p_0(r_0) \cong p_0(r_0)\beta^{5/2}x_0^5. \tag{62}$$

Now, let us try to describe this homogeneous isentropic compression by the self-similar motion. Using Eqs. (52) and (56), we immediately obtain

$$\begin{aligned} v(r,t) \equiv u(r_0, t) &= \dot{r} = r_0\dot{h}(t) = \frac{r\dot{h}(t)}{h(t)} \\ &= -\frac{r}{|t|}\frac{1 - \frac{|t|}{t_0}}{2(1 - \frac{|t|}{2t_0})} \Rightarrow -\frac{r}{2|t|} \quad , \end{aligned} \tag{63}$$

where the last expression is given for $t \to -0$. This equation shows that the gas motion in the final stage of the homogeneous compression must correspond to a certain point on the line $V = -\frac{1}{2}$ in the (V, Z) plane.

The corresponding Z-value can be obtained from the definition of Eq. (5), i.e.,

$$Z = \frac{\gamma p(r_0,t)}{\rho(r_0,t)}\frac{t^2}{r^2} = \frac{\gamma p_0(r_0)}{\rho_0(r_0)h^2(t)}\frac{t^2}{r^2}$$

$$\Rightarrow \begin{cases} \frac{1}{2}\left[\frac{r}{c_s(t_0|t|)^{1/2}}\right]^{-2} & \text{for} \quad \beta \ll 1 \ , \\ \frac{1}{12} & \text{for} \quad \beta \gg 1 \ , \end{cases} \tag{64}$$

where the last expressions are again for $t \to -0$.

The above equation suggests that a homogeneous isentropic compression can be the self-similar motion with $\delta = \frac{1}{2}$, i.e.,

$$\lambda = \frac{r}{c_s(t_0|t|)^{1/2}} \quad , \tag{65}$$

which takes values between zero and λ_0 defined by

$$\lambda_0 = \lambda(r = R) = (\frac{3}{2}\beta)^{1/2} . \tag{66}$$

The integral curve of this motion can hence be expressed by a line with $V = -\frac{1}{2}$ for $\beta \ll 1$, that starts from $Z = \infty$ and ends at $Z = \frac{1}{2}\beta^{-2}$, while it corresponds to one point ($V = -\frac{1}{2}$, $Z = \frac{1}{12}$) for $\beta \gg 1$.

The density and pressure can be represented in a the following self-similar forms, respectively:

$$\rho(r,t) \equiv \rho(r_0,t) = \begin{cases} \rho_0(0)\,\dfrac{c_s^3 t_0^3 \lambda^3}{2^{3/2} r^3} & \text{for } \beta \ll 1, \\ \rho_0(0)\,\dfrac{c_s^3 t_0^3 \lambda^6}{(2\cdot 3^{1/2})^3 r^3} & \text{for } \beta \gg 1, \end{cases} \tag{67}$$

$$p(r,t) \equiv p(r_0,t) = \begin{cases} p_0(0)\,\dfrac{c_s t_0^3 \lambda}{2^{5/2} r t^2} & \text{for } \beta \ll 1, \\ p_0(0)\,\dfrac{c_s t_0^3 \lambda^6}{(2\cdot 3^{1/2})^5 r t^2} & \text{for } \beta \gg 1, \end{cases} \tag{68}$$

In other words, the motion followed by a homogeneous isentropic compression can be represented by the self-similar motion with $k = 0$, $s = 0$ and $\delta = \frac{1}{2}$ in the final stage of compression. Here, it may be noted that every point on the line $V = -\frac{1}{2}$ is the singular point as seen from Eq. (6).

A more detailed treatment would be needed for complete description of the homogeneous isentropic compression by the self-similarity analysis. This problem will be studied, together with the problem discussed in the previous subsection, in a separate paper.

V. SUMMARY AND CONCLUSIONS

We have studied the implosion process induced by laser-heated ablation by means of the self-similarity analysis. Particular attention has been paid to the possibility of the existence of the self-similar solution which reproduces the implosion process.

At first, the actual details of the self-similar analysis was reproduced by following Sedov. The gas compression by a single shock was analysed by assuming its dynamics as a self-similar motion. A gas compression beyond the compression ratio of about 10 was shown to be impossible for $t < 0$ by a single shock.

Discussions have been made on the possibility that a self-similar motion can reproduce the gas motion accompanied by extremely high compression. The following conclusions have been drawn:

(1) The implosion process accompanied by a sequence of the shocks can not be represented by a self-similar motion under the assumption of the uniform initial gas state and the extremely strong shock.

(2) The gas motion followed by a homogeneous isentropic compression can be reproduced by a self-similar motion with $k = 0$, $s = 0$ and $\delta = \frac{1}{2}$, in the final stage of compression.

Further studies will be needed for the following two cases from the standpoint of the self-similarity analysis:

(1) The first is the case where the shocks proceed in the gas with a spatial dependence of density ($\rho = ar^{2/\delta-2}$).

(2) The second is the homogeneous isentropic compression which has not completely been treated in the present paper.

REFERENCES

1) J. Nuckolls, T. Wood, A. Thiessen, and G. Zimmerman; Nature, 236, 139 (1972).
2) E. B. Goldman; Plasma Phys., 15, 289 (1972).
3) K. Brueckner and S. Jorna; Rev. Mod. Phys., 46, 325 (1974).
4) R. E. Kidder; Nuclear Fusion, 14, 53 (1974) and 14, 797 (1974).
5) R. J. Mason and R. L. Morse; Phys. Fluids, 18, 814 (1975).
6) L. I. Sedov; "Similarity and Dimensional Method in Mechanics", Academic Press, New York (1959).
7) K. Oswatitsh and G. Kuerti; "Gas Dynamics", Academic Press, New York

V. SUMMARY AND CONCLUSIONS

We have studied the implosion process induced by laser-heated ablation by means of the self-similarity analysis. Particular attention has been paid to the possibility of the existence of the self-similar solution which reproduces the implosion process.

At first, the actual details of the self-similar analysis was reproduced by following Sedov. The gas compression by a single shock was analysed by assuming its dynamics as a self-similar motion. A gas compression beyond the compression ratio of about 10 was shown to be impossible for $t < 0$ by a single shock.

Discussions have been made on the possibility that a self-similar motion can reproduce the gas motion accompanied by extremely high compression. The following conclusions have been drawn:

(1) The implosion process accompanied by a sequence of the shocks can not be represented by a self-similar motion under the assumption of the uniform initial gas state and the extremely strong shock.

(2) The gas motion followed by a homogeneous isentropic compression can be reproduced by a self-similar motion with $k = 0$, $s = 0$ and $\delta = \frac{1}{2}$, in the final stage of compression.

Further studies will be needed for the following two cases from the standpoint of the self-similarity analysis:

(1) The first is the case where the shocks proceed in the gas with a spatial dependence of density ($\rho = ar^{2/\delta-2}$).

(2) The second is the homogeneous isentropic compression which has not completely been treated in the present paper.

REFERENCES

1) J. Nuckolls, T. Wood, A. Thiessen, and G. Zimmerman; Nature, 236, 139 (1972).
2) E. B. Goldman; Plasma Phys., 15, 289 (1972).
3) K. Brueckner and S. Jorna; Rev. Mod. Phys., 46, 325 (1974).
4) R. E. Kidder; Nuclear Fusion, 14, 53 (1974) and 14, 797 (1974).
5) R. J. Mason and R. L. Morse; Phys. Fluids, 18, 814 (1975).
6) L. I. Sedov; "Similarity and Dimensional Method in Mechanics", Academic Press, New York (1959).
7) K. Oswatitsh and G. Kuerti; "Gas Dynamics", Academic Press, New York

(1956).

8) J. N. Bradley; "Shock Waves in Chemistry and Physics", John Wiley & Sons Inc., New York (1962).

9) G. Guderly; Luftfahrtforshung, 19, 302 (1942).

10) For example, K. O. Friedrichs; "Advanced Ordinary Differential Equations," Gordon and Breach Science Publishers, New York, London, Paris (1968).

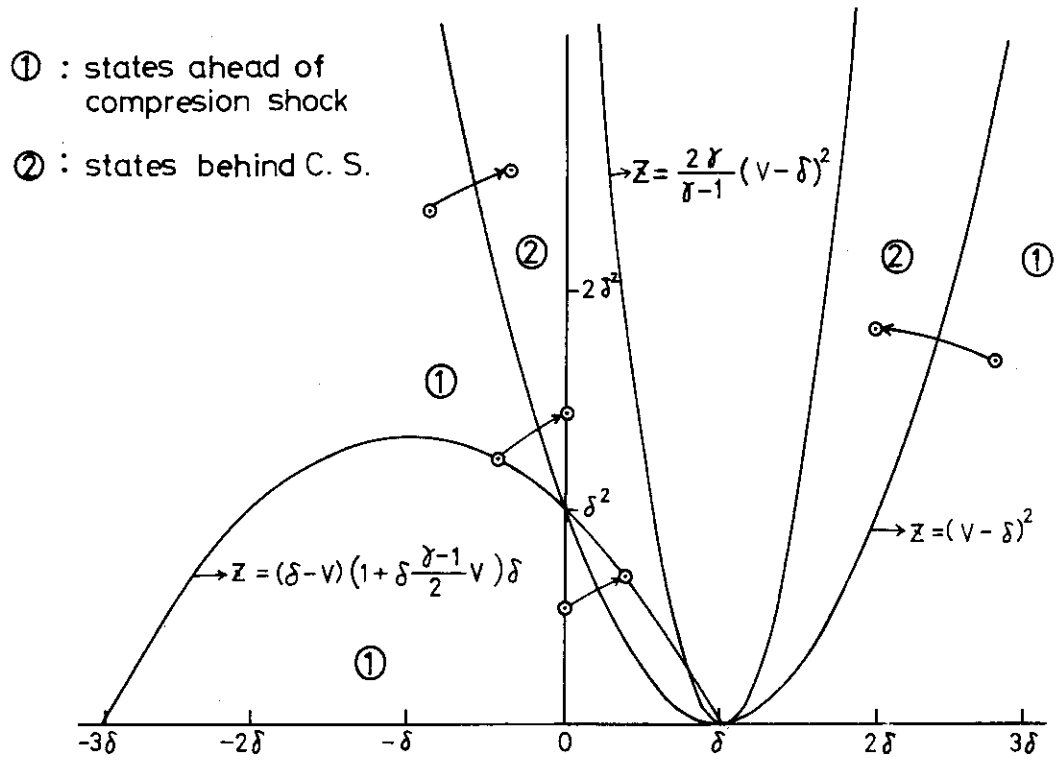

Fig. 1. Possible transformations from (V_1, Z_1) to (V_2, Z_2).

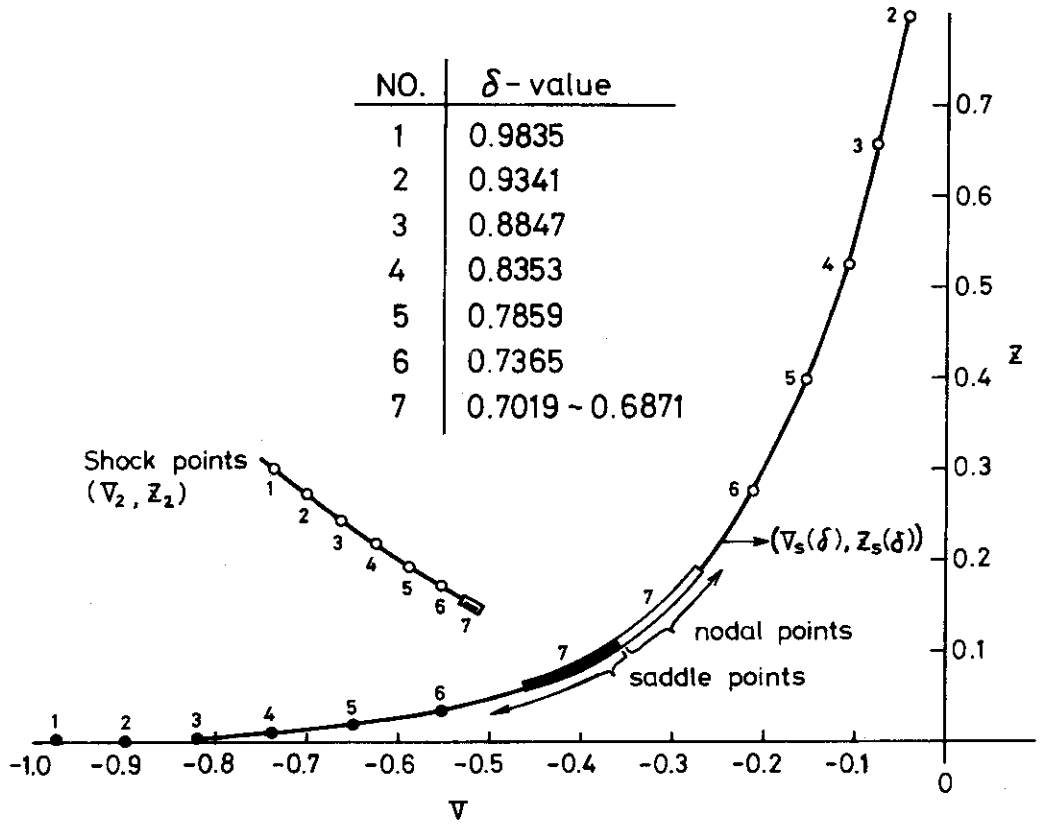

Fig. 2. Dependence of shock, saddle and nodal points on δ-value.

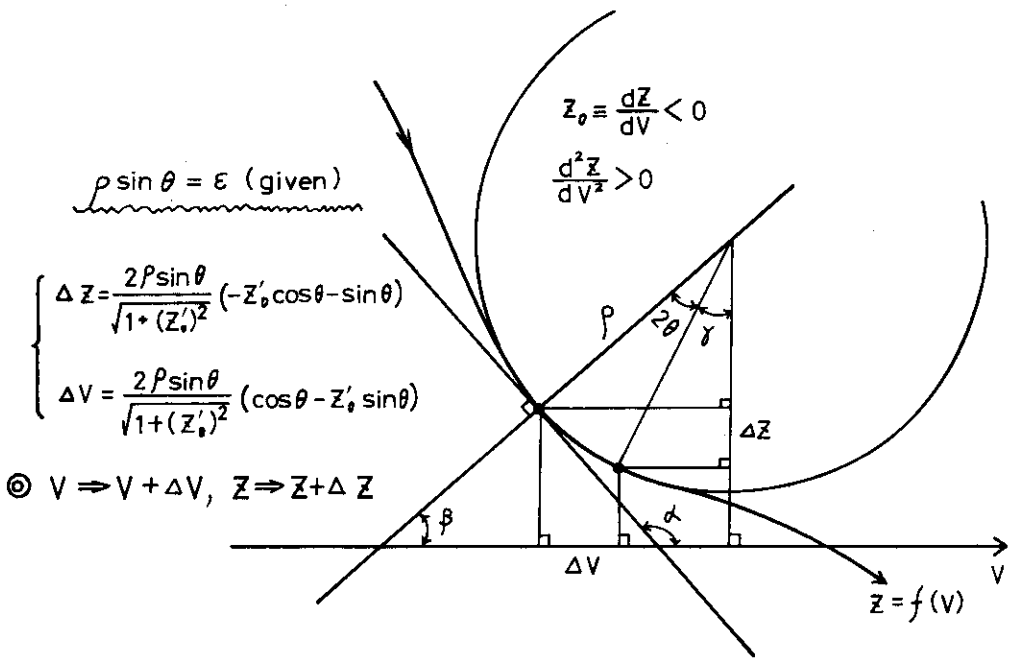

Fig. 3. Numerical method for obtaining integral curves.

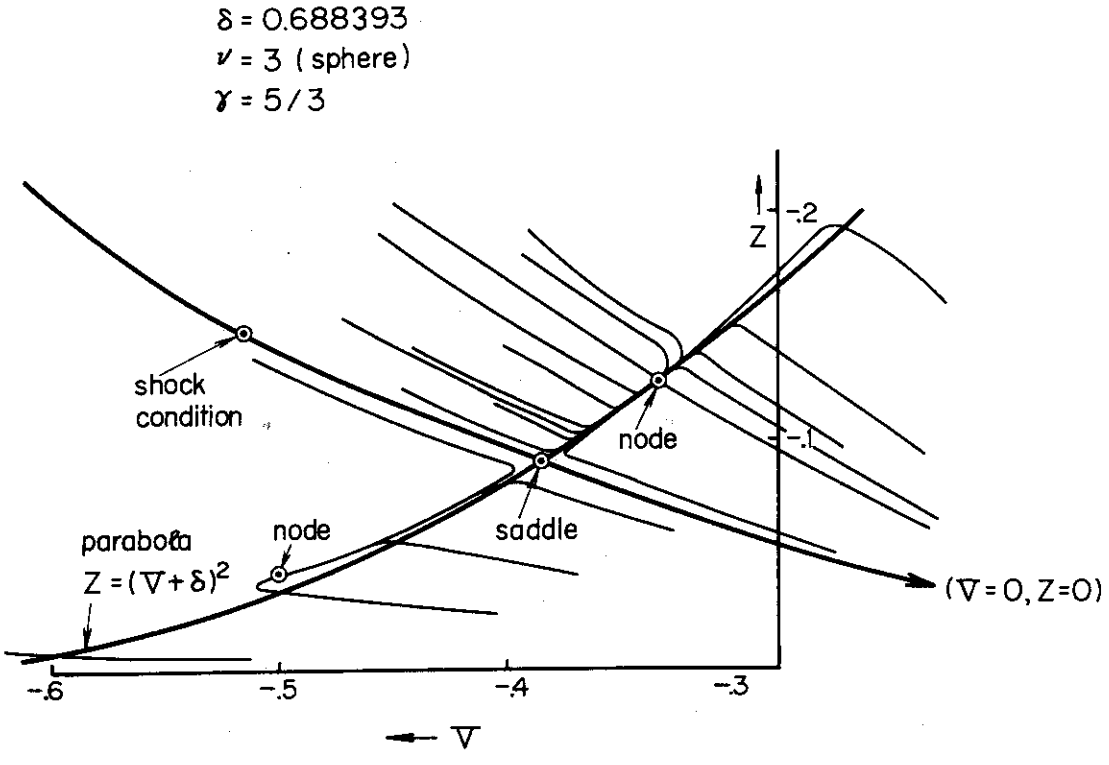

Fig. 4. The family of integral curves for k=-3, s=0, ν=3, δ=0.68839 and γ=5/3

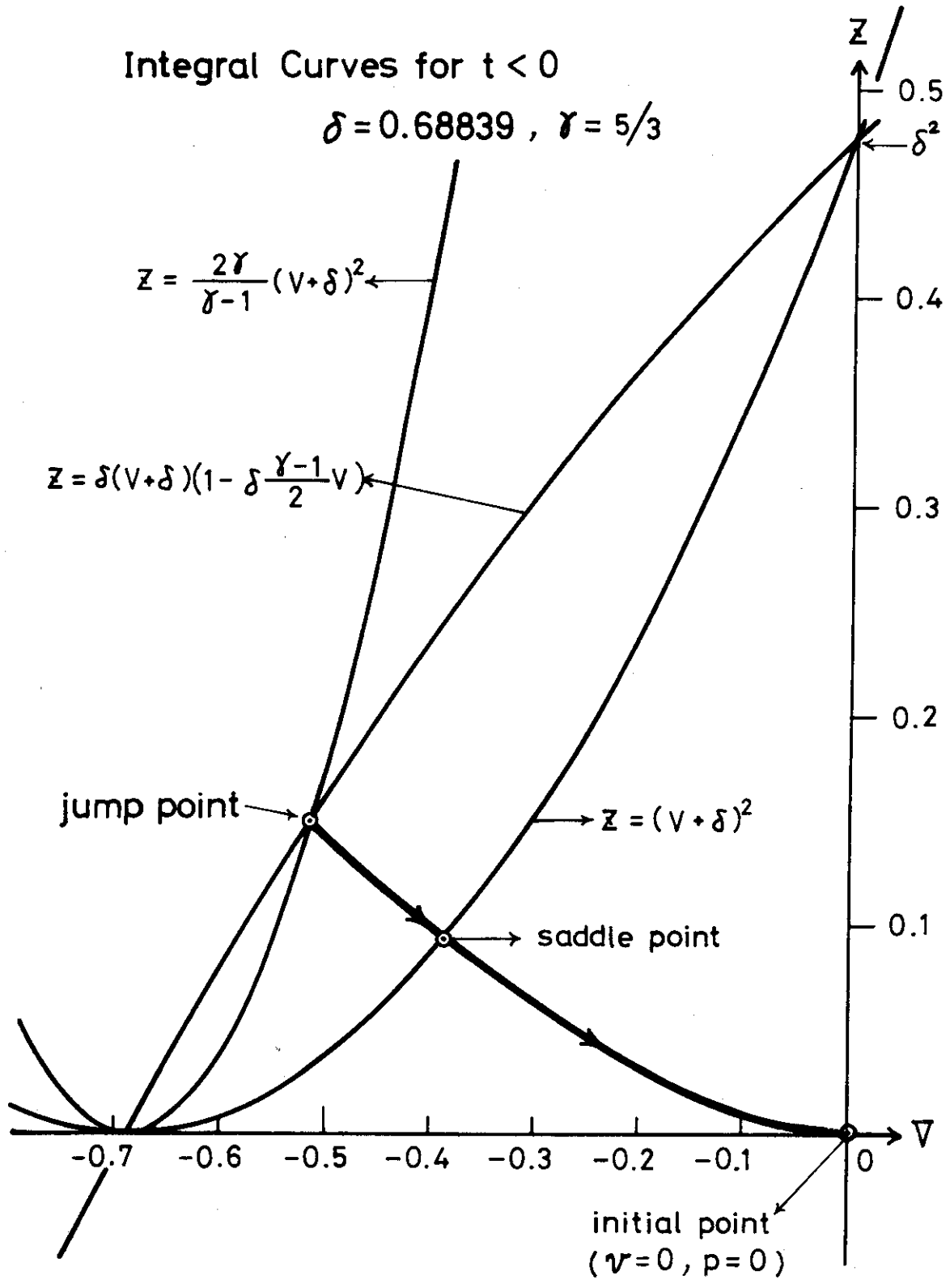

Fig. 5. The integral curve for implosion process (t<0).

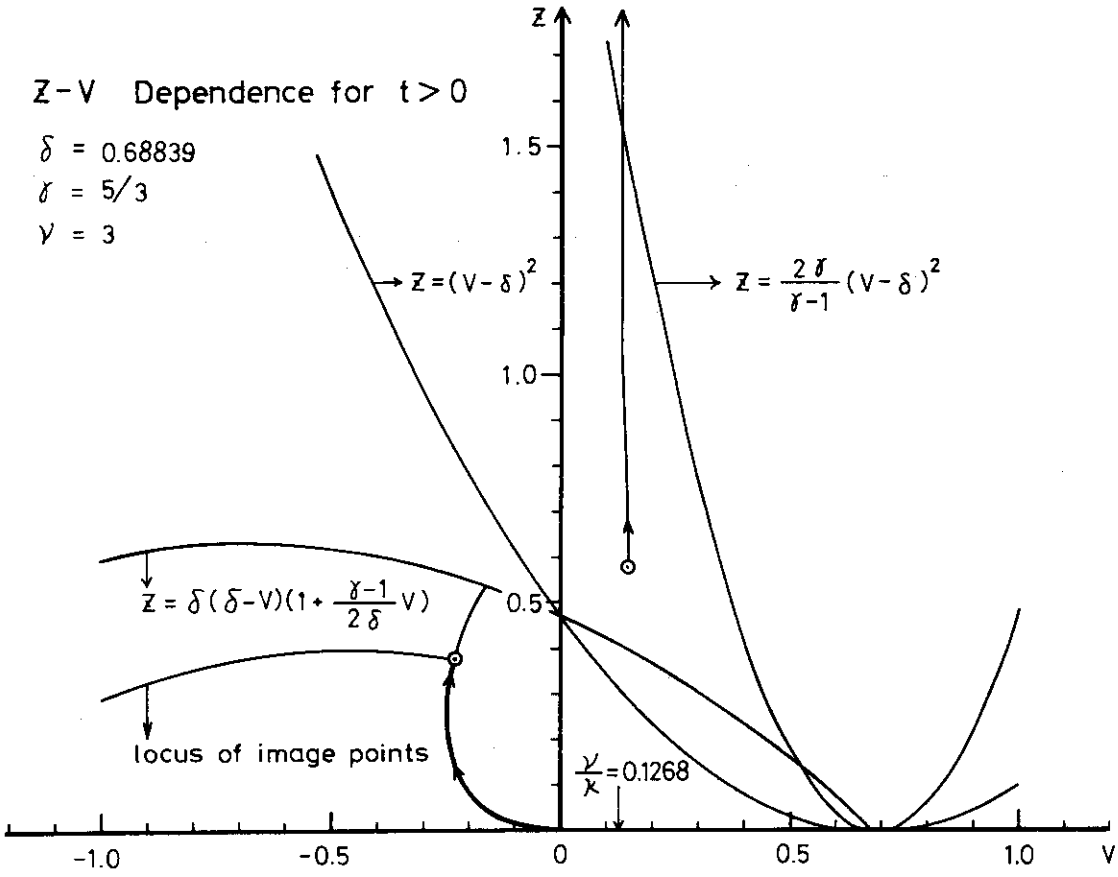

Fig. 6 The integral curve for explosion process (t>0).

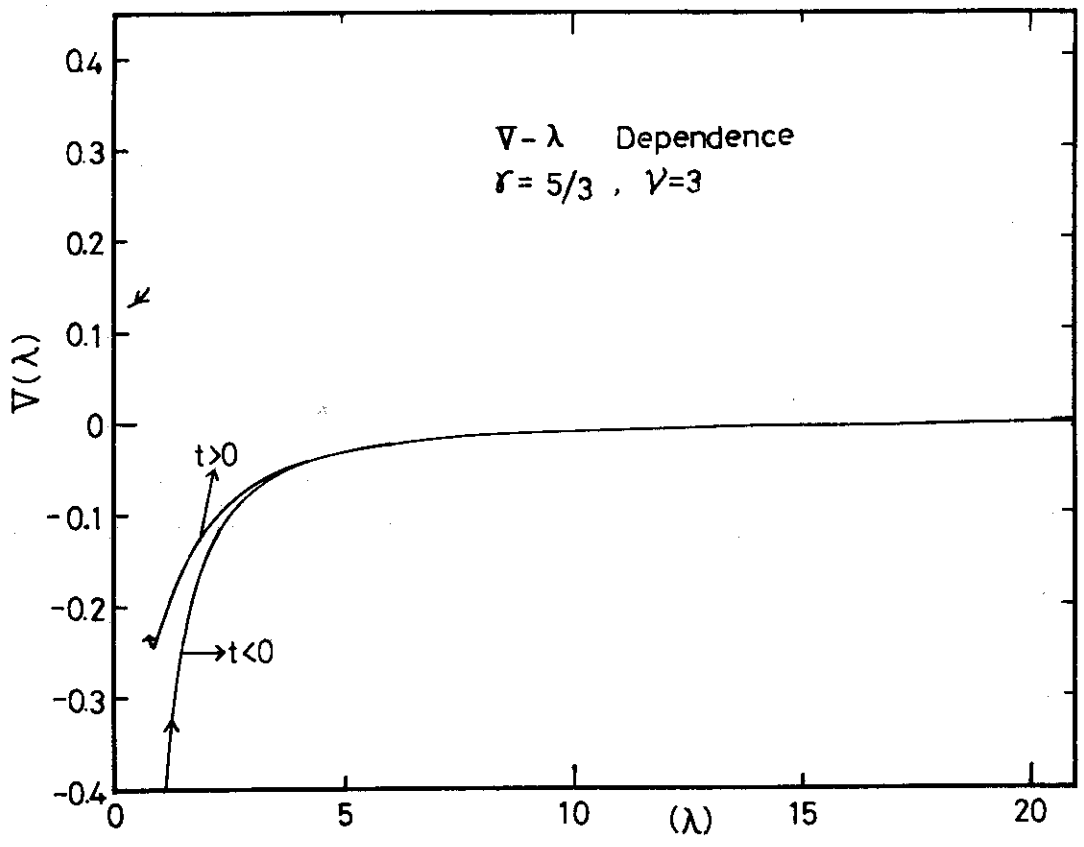

Fig. 7 The λ-dependence of V.

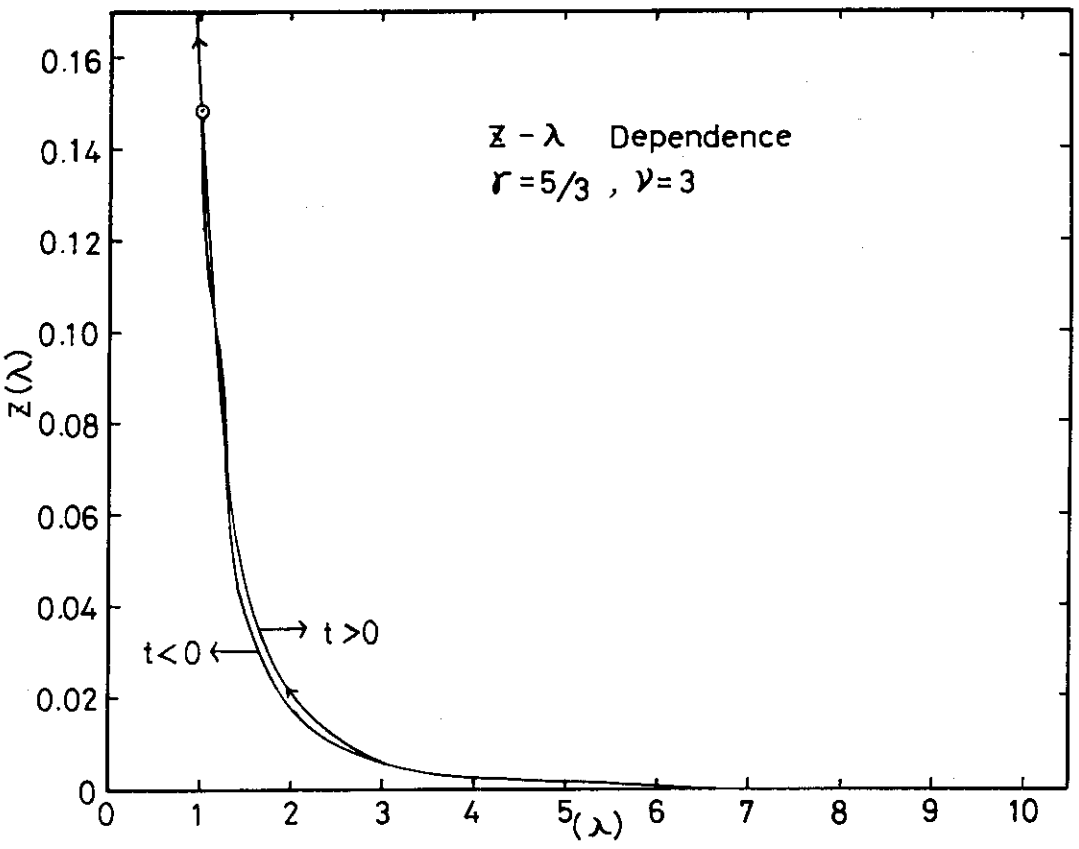

Fig. 8 The λ-dependence of Z.

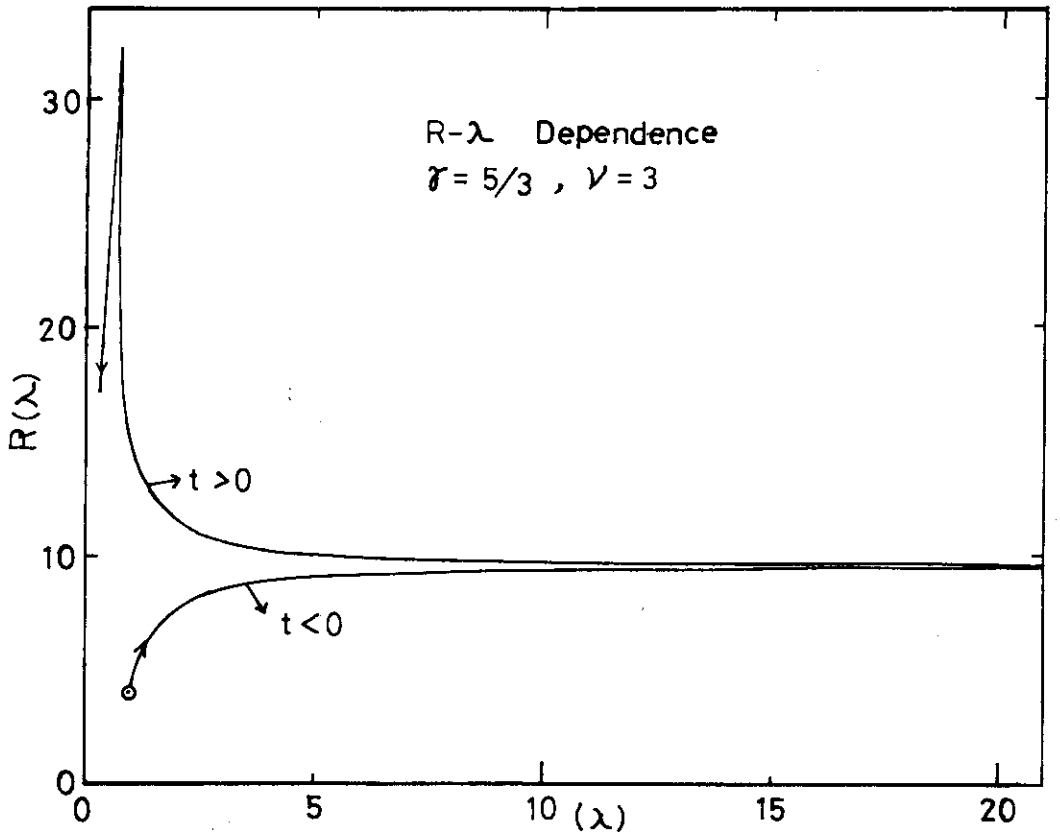

Fig. 9 The λ-dependence of R.

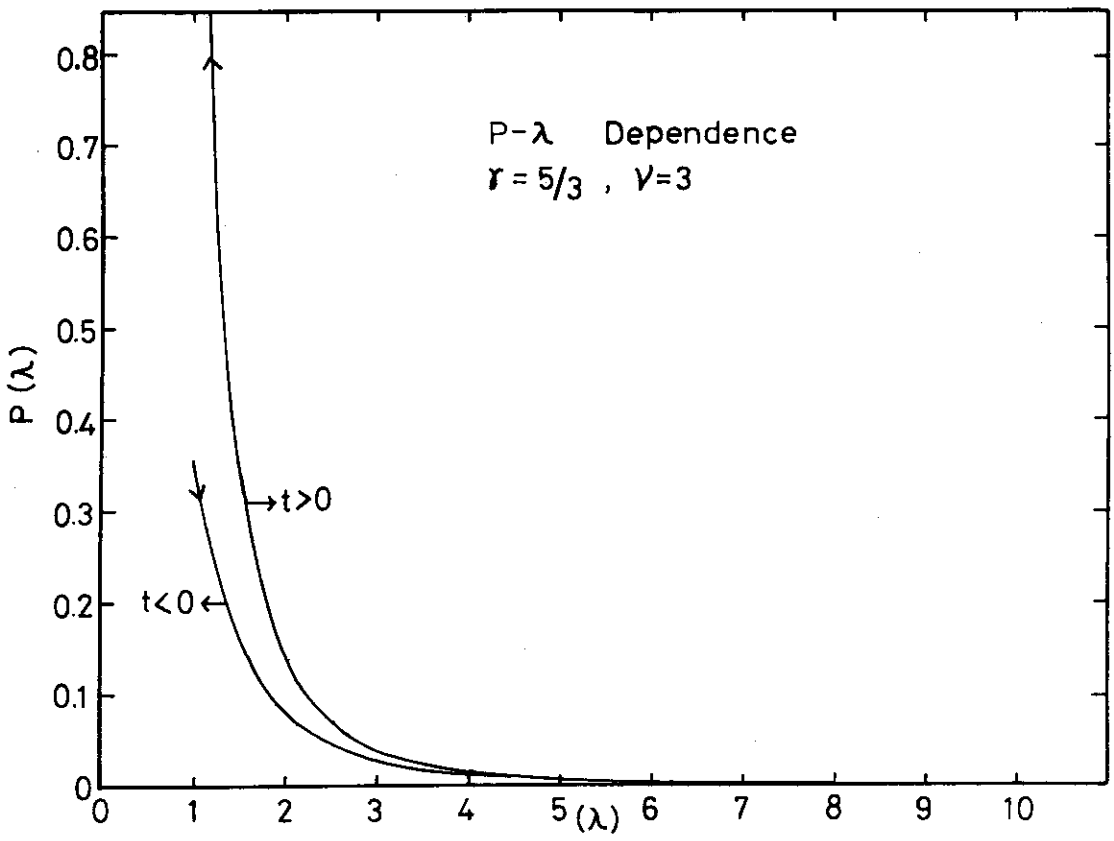

Fig. 10 The λ-dependence of P.

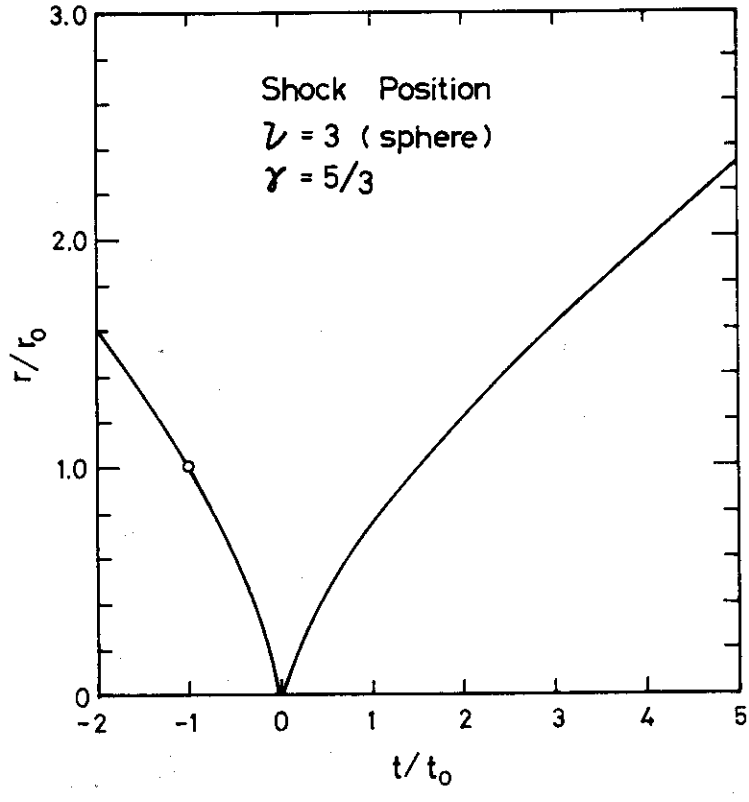

Fig. 11 Shock position as function of time.

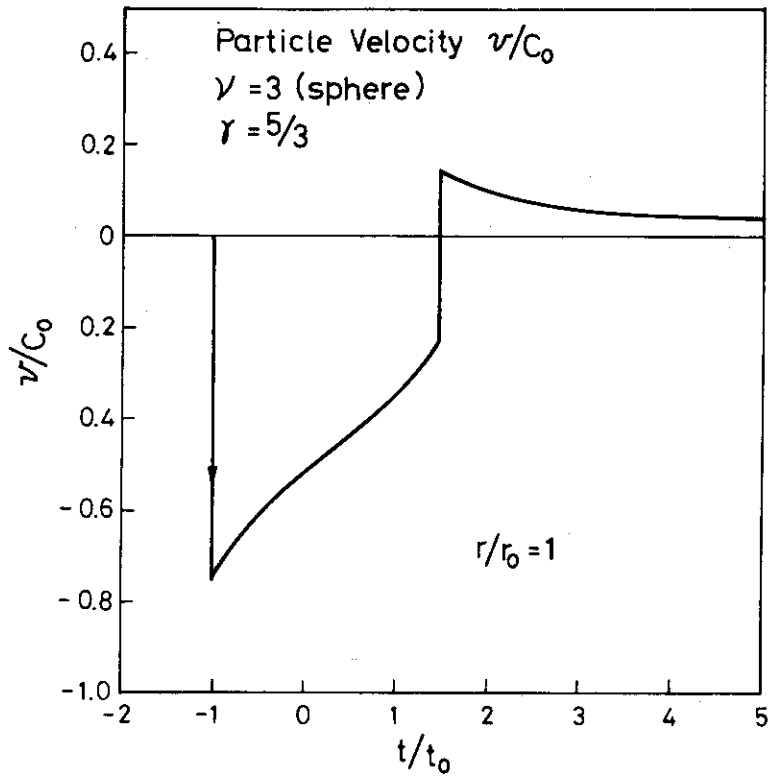

Fig. 12 Particle velocity as function of time.

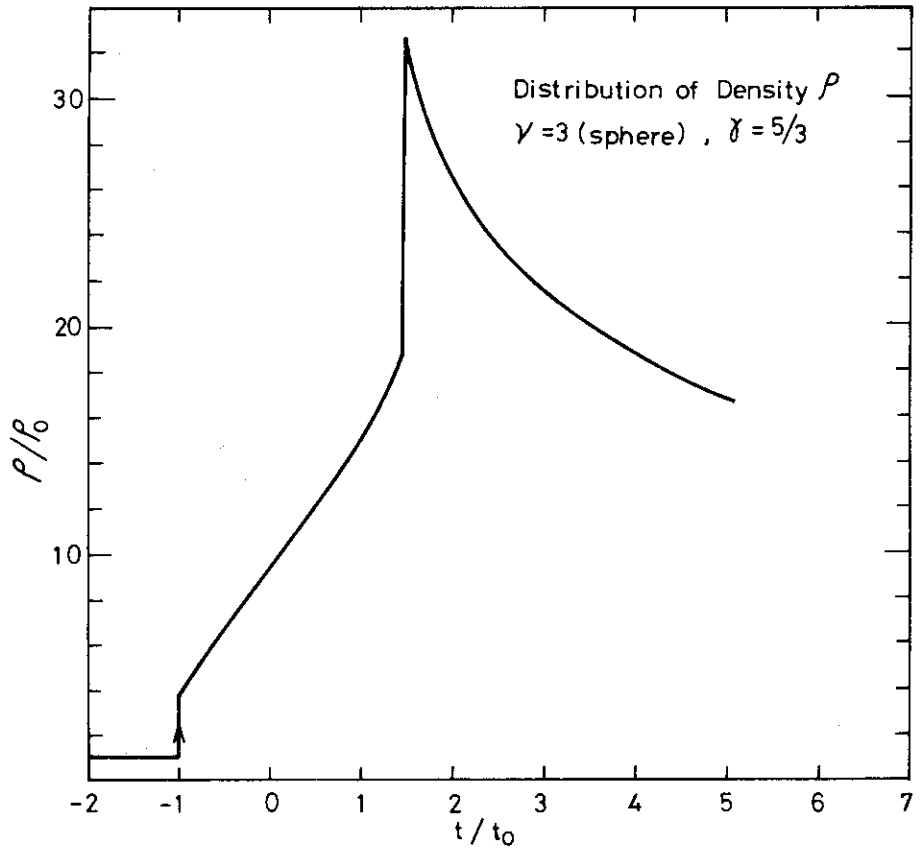

Fig. 13 Distribution of dencity ρ (r/r_0=1).

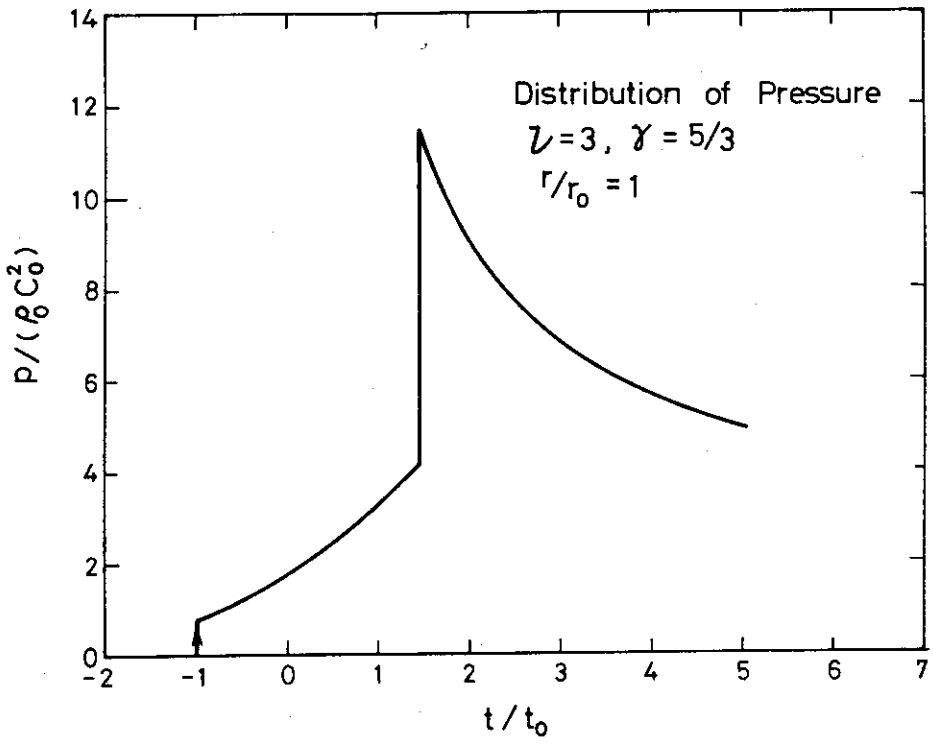

Fig. 14 Distribution of pressure p (r/r_0=1).

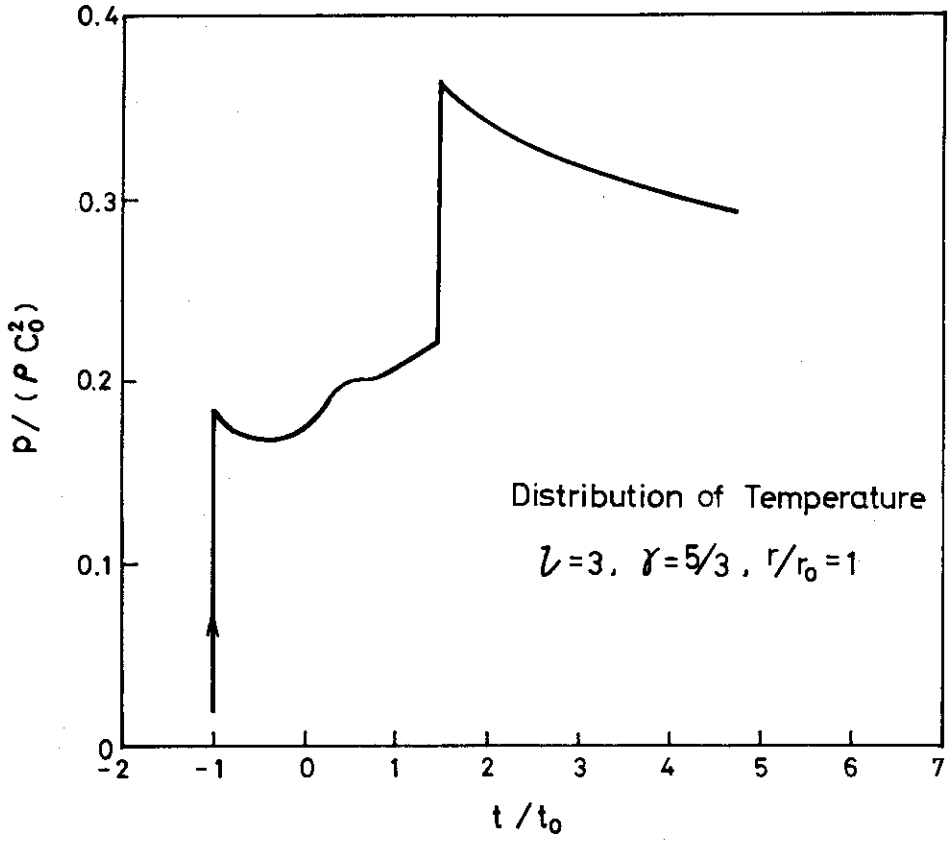

Fig. 15 Distribution of temperature ($p/(\rho c_0^2)$; r/r_0=1).

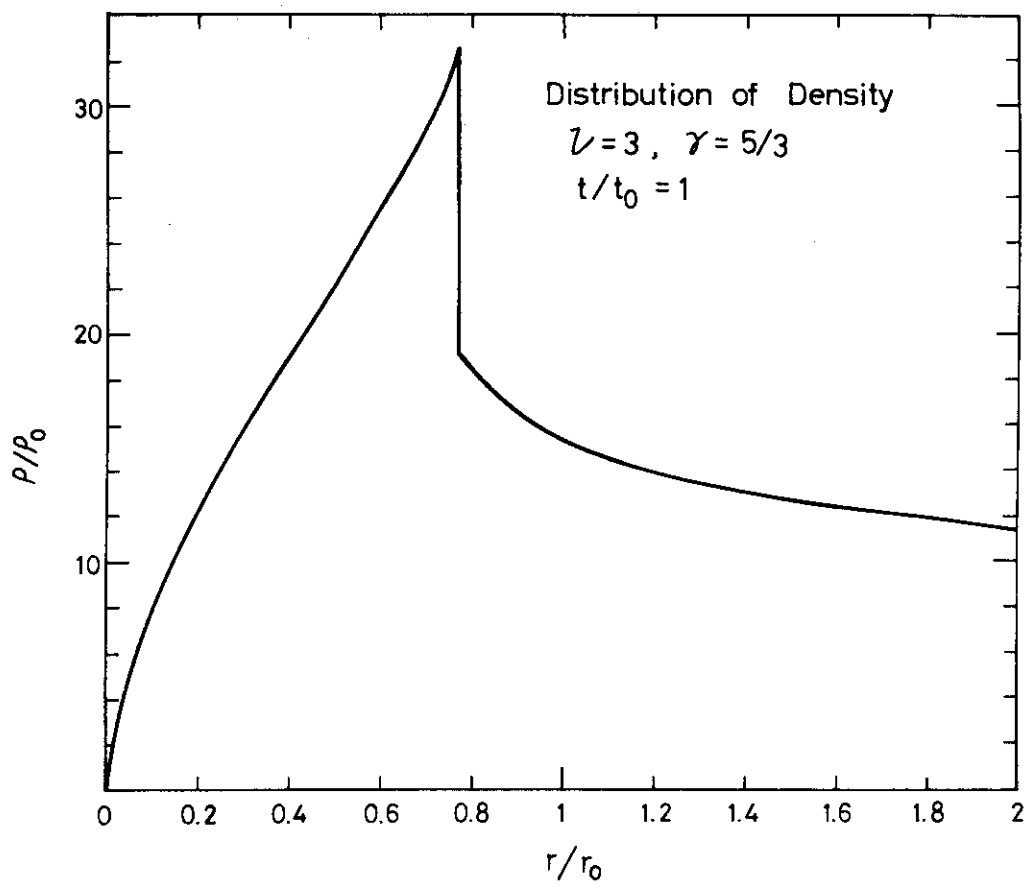

Fig. 16 Radial distribution of density for t>0.

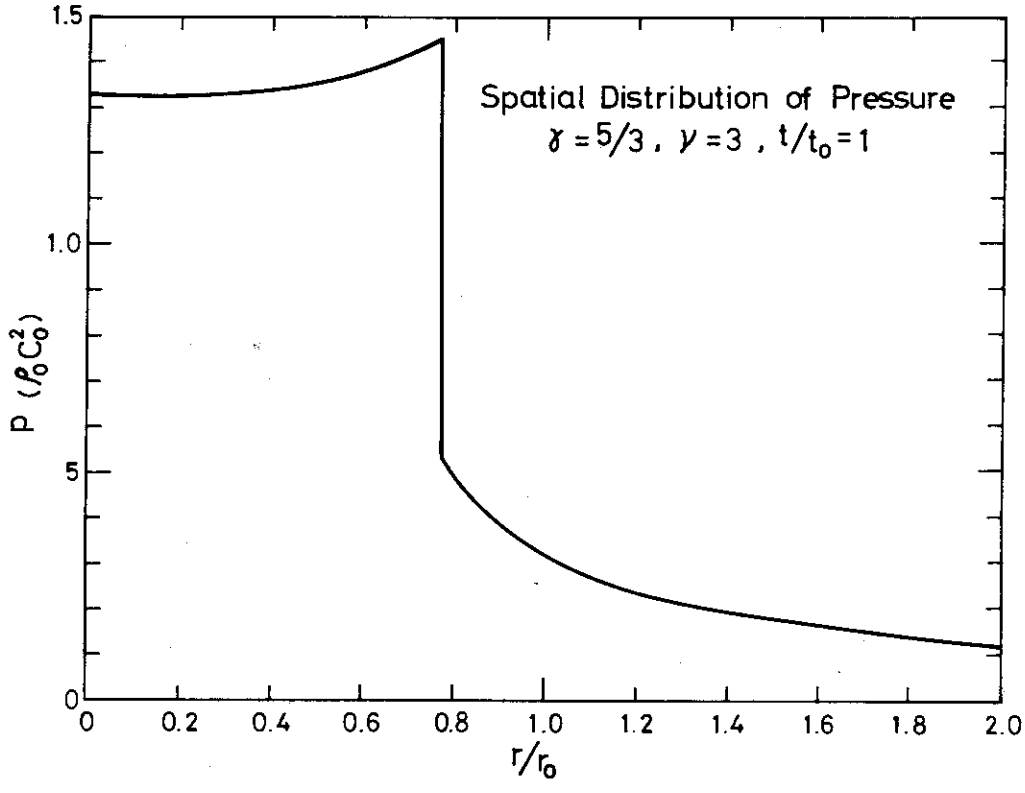

Fig. 17 Radial distribution of pressure for t>0.

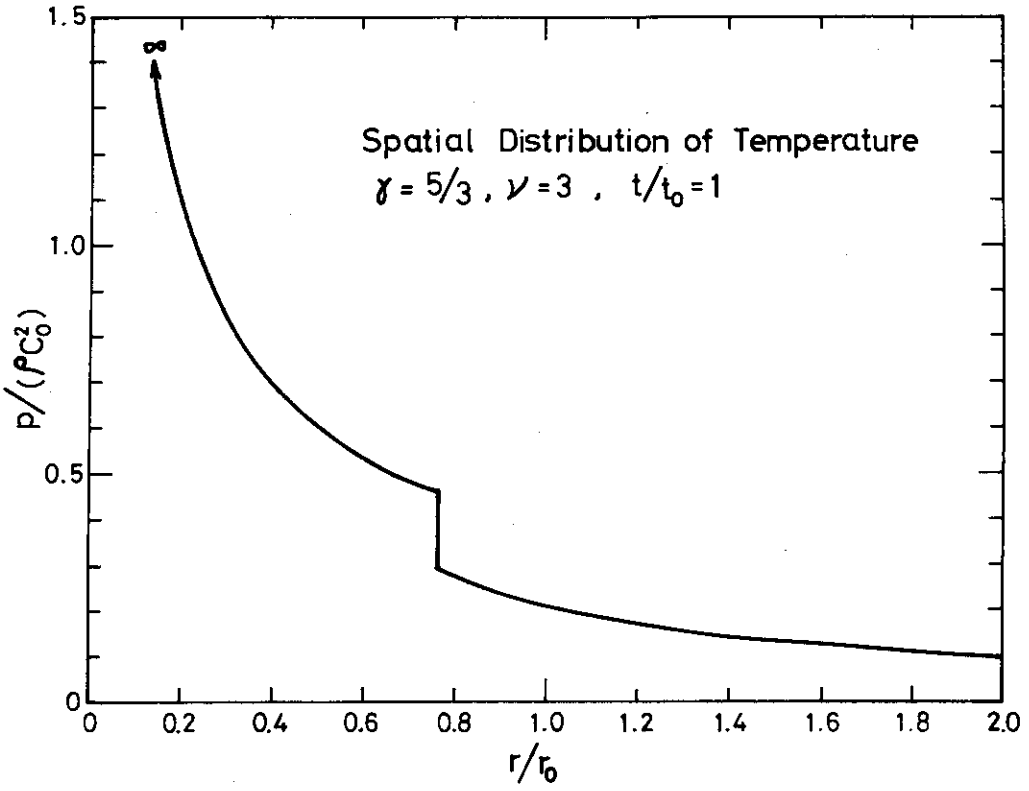

Fig. 18 Radial distribution of temperature for t>0.

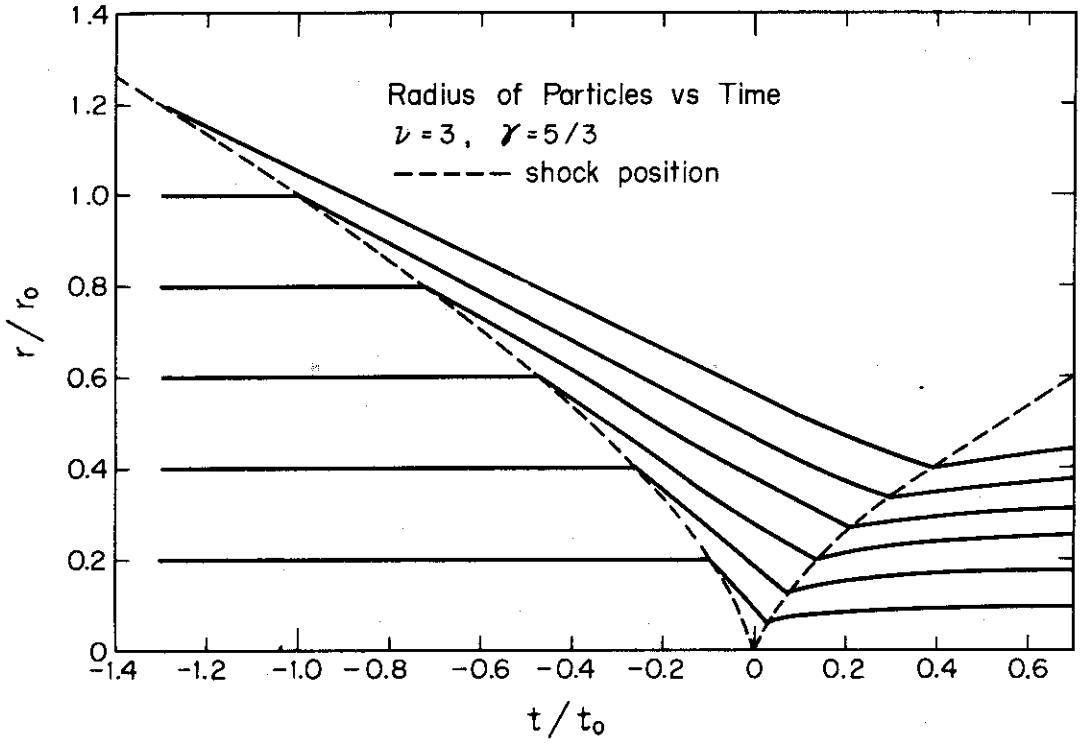

Fig. 19 Reduced radius r/r_0 of fluid particles versus reduced time t/t_0.

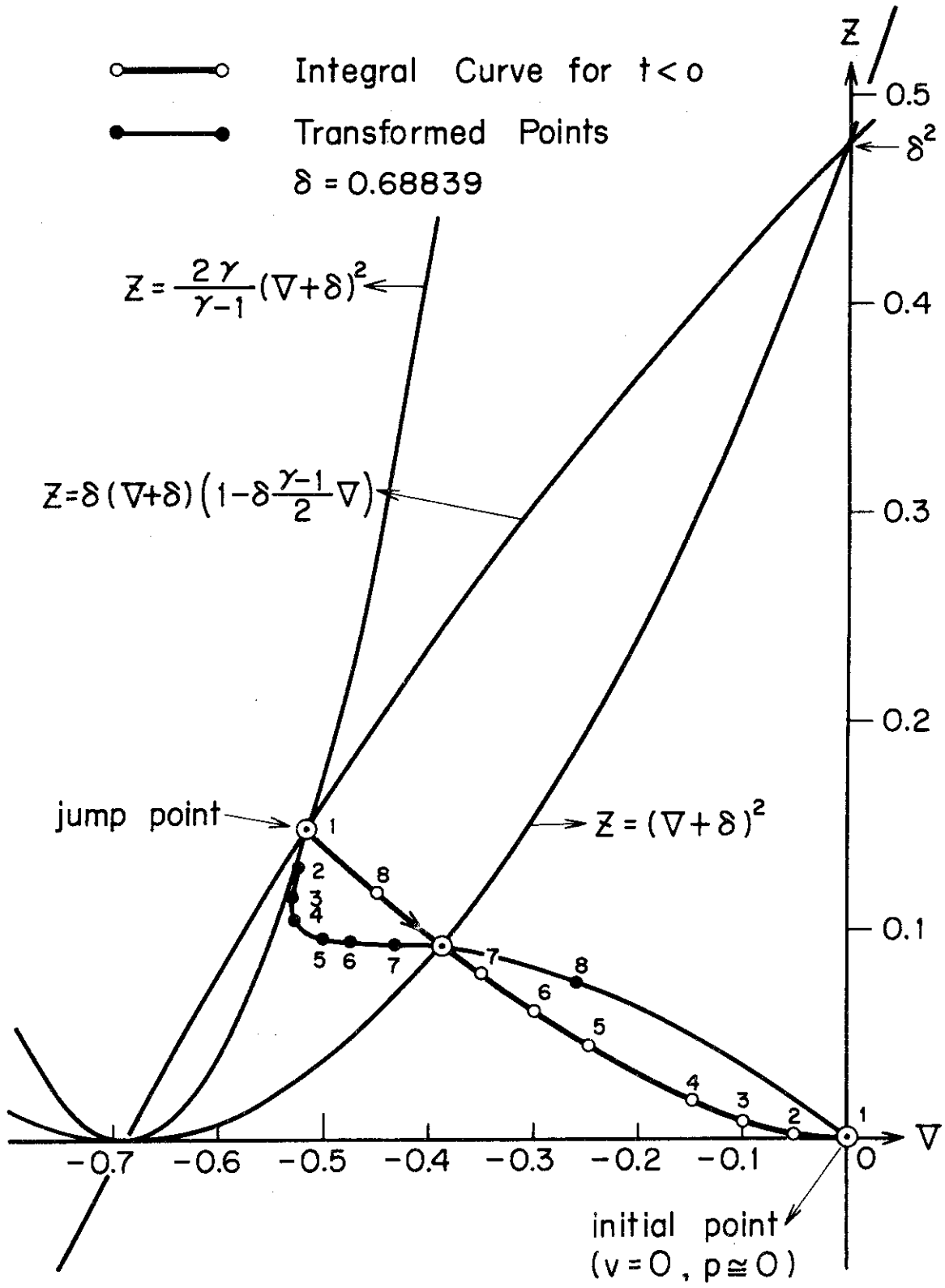

Fig. 20 Locus of image points obtained from the points on integral curve through shock transformation